

## Improved Cycling Performance of Directly Lithiated MoO<sub>3</sub> Nanobelts

Liqiang Mai<sup>1,2</sup>, Bin Hu<sup>1</sup>, Yanyuan Qi<sup>1</sup>, Ying Dai<sup>1</sup>, Wen Chen<sup>1,\*</sup>

<sup>1</sup>State Key Laboratory of Advanced Technology for Materials Synthesis and Processing, Institute of Materials Science and Engineering, Wuhan University of Technology, Wuhan, 430070, China

<sup>2</sup>School of Materials Science and Engineering, Georgia Institute of Technology, Atlanta, Georgia 30332-0245, USA.

\*E-mail: [chenw@whut.edu.cn](mailto:chenw@whut.edu.cn), [imai6@mail.gatech.edu](mailto:imai6@mail.gatech.edu)

Received: 29 November 2007 / Accepted: 12 December 2007 / Online published: 20 December 2007

---

Lithiation modification of MoO<sub>3</sub> nanobelts was carried out by a simple hydrothermal method. The structure and morphology of the directly lithiated MoO<sub>3</sub> nanobelts were characterized by XRD and SEM. The results show that, compared to that of pristine MoO<sub>3</sub> nanobelts, the size of lithiated MoO<sub>3</sub> nanobelts with a width of about 200 nm and a length of 5~8 μm decreases, while preserving crystal structure and belt-shape morphology. The lithiated MoO<sub>3</sub> nanobelts exhibit good cycling capability, with a capacity retention rate of 50% after 39 cycles, while the non-lithiated nanobelts retain only 26.5%. It is proposed that the Li<sup>+</sup> ions occupy the interstitial site of MoO<sub>3</sub> lattice which can stabilize the structure and reduce the electrostatic interaction between MoO<sub>3</sub> layer and Li<sup>+</sup> ions in the interlayer during the discharge, resulting in the improvement of electrochemical performance.

---

**Keywords:** Molybdenum trioxide nanobelts, Lithiation modification, Electrochemical performance, Cycling property

### 1. INTRODUCTION

Stable high-capacity rechargeable lithium-ion cells are considered to be the most advanced energy storage systems and are demanded in portable and low-power, long-life equipments. Research on cathode materials is very intensive as there is a strong desire to find alternatives to cobalt-based oxides used in commercial cells because of their high cost and toxicity. Moreover, 1-D nanomaterials with layered structure have emerged as among the most promising due to their better properties than that of traditional bulk materials [1], and doping is also an effective method to improve the performance [2].

MoO<sub>3</sub> has been investigated extensively as a key material for fundamental research, and can be used in a wide variety of application because of its properties as field emitters [3], optical devices, thermoelectric-materials [4], catalysts [5], sensors [6], lubricants [7], and electrochemical storage [8]. As the thermodynamically stable phase, orthorhombic MoO<sub>3</sub> ( $\alpha$ -type) can be considered as a layered structure in parallel to (010). Each layer is composed of two sub-layers, each of which is formed by corner-shared octahedra along [001] and [100], the two sub-layers stack together by sharing the edges of the octahedra along [001]. An alternate stack of these layered sheets along [010] will lead to the formation of  $\alpha$ -MoO<sub>3</sub>, where van der Waals interaction is the major binding between the piled sheets, the special anisotropy structure of  $\alpha$ -MoO<sub>3</sub> is facile to form belt-like morphology.

As one of potential excellent cathode materials, MoO<sub>3</sub> nanobelts had been synthesized using hydrothermal method [9], but the electrochemical test indicated that the layered structure of MoO<sub>3</sub> would be destroyed in the process of Li<sup>+</sup> ion insertion/extraction, and the reversible capacity decreased fast. For inhibiting the capacity decay, the method of polymer intercalation such as PEO, PMMA is investigated to keep the layered structure intact during the cycles, and it is shown that lithiation is also helpful for improving the cathodic behavior and thermal stability in the charged state [10], so herein a novel and simple hydrothermal method was used to synthesize lithiated MoO<sub>3</sub> nanobelts, and the results show the lithiated MoO<sub>3</sub> nanobelts have more stable electrochemical performance compared to the pristine one.

## 2. EXPERIMENTAL PART

40 ml H<sub>2</sub>O<sub>2</sub> (30%) was agitated rapidly and added 4 g molybdenum powder slowly under water cooling until the clear orange sol was obtained, subsequently LiCl powder was added into the sol, and stirred for 12 hours in ambient temperature to remove the residual H<sub>2</sub>O<sub>2</sub>. The orange sol was directly transferred to a Teflon-lined autoclave and kept at 180 °C for 48 hours. Next, the autoclave was left to cool down in air, the solid precipitate was filtered out and rinsed with deionised water at least five times to remove the LiCl adsorbed on the surface of the nanobelts. The light blue product was obtained after drying at 80 °C for 4 h. The pristine MoO<sub>3</sub> nanobelts were synthesized using direct hydrothermal reaction of peroxomolybdic acid sols without adding LiCl [1].

X-ray diffraction (XRD) measurement was performed using a D/MAX-III X-ray diffractometer. Scanning electron microscopy (SEM) images were collected with JSM-5610 and FES-EM LEO 1530. The electrochemical properties were studied with a multichannel battery testing system. Batteries were fabricated using a lithium pellet as negative electrode; 1 M solution of LiPF<sub>6</sub> in ethylene carbon (EC)/dimethyl carbonate (DMC) as electrolyte and a pellet made of the nanobelts, acetylene black and PTFE in a 10:7:1 ratio as the positive electrode. The cyclic voltammograms (CV) were measured at the scan rate of 0.5 mV/s with an Autolab model PGSTAT30 (GPES/FRA) potentiostat/galvanostat interfaced to a computer.

### 3. RESULTS AND DISCUSSION

#### 3.1 XRD Analysis

The XRD pattern of lithiated  $\text{MoO}_3$  nanobelts is compared with that of pristine nanobelts in Fig. 1. Both of the samples can be indexed on the basis of an orthorhombic cell with crystallographic parameters of  $a=3.962\text{\AA}$ ,  $b=13.85\text{\AA}$ ,  $c=3.697\text{\AA}$  (JCPDS No. 05-0508) which correspond with the standard  $\alpha\text{-MoO}_3$  pattern. Compared to the pristine nanobelts, the increase of relative intensity of (110) and (021) peaks show that lithiation has certain influence on the crystallization of  $\text{MoO}_3$  nanobelts, but the appearance of no new peaks conforms that the crystal structure is still kept as orthorhombic phase. Notably, lithiation by this method does not expand the interlayer spacing, which is different from the previous report [11]. Although the radius discrepancy between  $\text{Li}^+$  (60 pm) and  $\text{Mo}^{6+}$  (62 pm) is not remarkable, it is difficult for  $\text{Li}^+$  ions to replace  $\text{Mo}^{6+}$  ions because of the difference in ion valence, so probably the  $\text{Li}^+$  ions had been incorporated into the interstitial sites of  $\text{MoO}_3$  lattice, and this conclusion is conformed by cyclic voltammogram later.

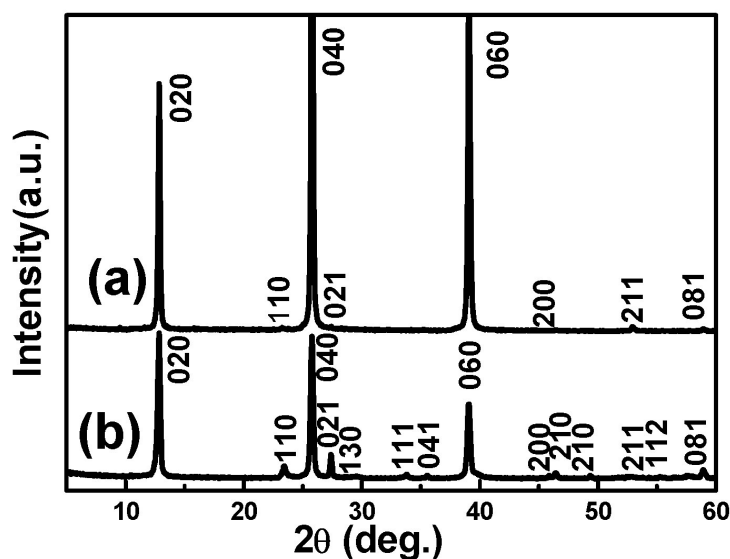


**Figure 1.** XRD patterns of pristine  $\text{MoO}_3$  nanobelts (a) and lithiated  $\text{MoO}_3$  nanobelts(b)

#### 3.2 SEM Analysis

The size and morphology of the resulting products were examined by scanning electron microscopy (SEM). As shown in Fig. 2, lithiation has no influence on belt-like morphology, and the rectangular cross sections are visible. But the width around 200 nm is smaller than that of pristine  $\text{MoO}_3$  nanobelts and the length also decreases to 5~8  $\mu\text{m}$ , and some fracture nanobelts with lengths of 200~400 nm can be seen in Fig. 2b clearly.

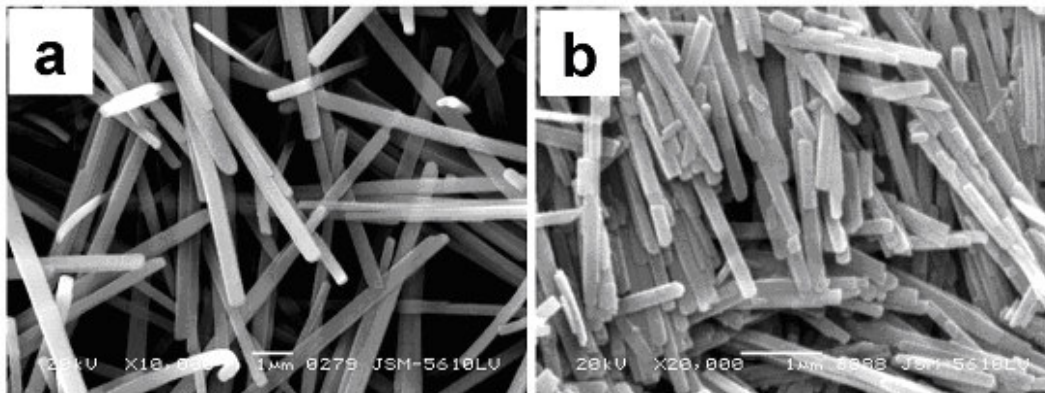


**Figure 2.** SEM of pristine MoO<sub>3</sub> nanobelts (a) and lithiated MoO<sub>3</sub> nanobelts (b)

3.3 Electrochemical Investigation

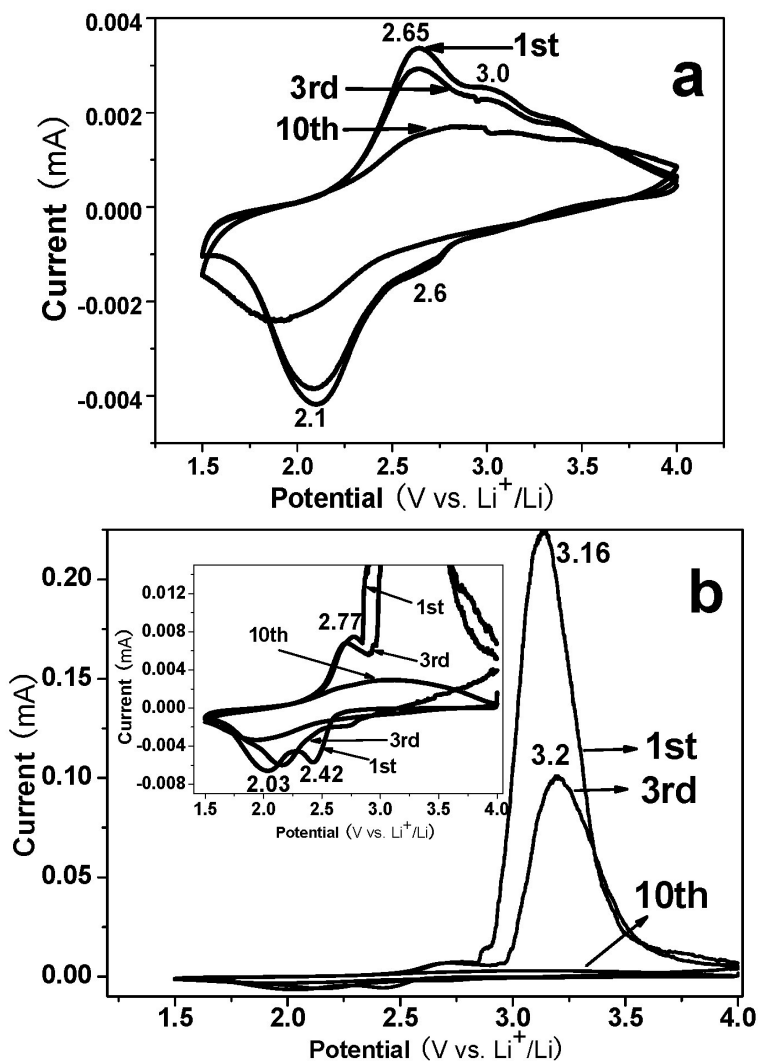


**Figure 3.** Cyclic voltammograms of pristine MoO<sub>3</sub> nanobelts (a) and lithiated MoO<sub>3</sub> nanobelts (b). The inset is the local enlarging graphs of Fig. 3b

Fig. 3a and 3b show the cyclic voltammograms of the pristine and lithiated MoO<sub>3</sub> nanobelts, respectively, in which the first, third and tenth cycle curves are plotted. The inset is the local enlarging graph of Fig. 3b. There are two sets of (cathodic, anodic) current peaks appearing at around the potential (V) of (2.03, 2.77) and (2.42, 3.16) in the first cycle curve of the lithiated MoO<sub>3</sub> nanobelts (Fig. 3a), and the two sets of peaks can be assigned to the insertion/extraction of Li<sup>+</sup> ions between the MoO<sub>6</sub> octahedron interlayers and intralayers, respectively [12]. Obviously, the anodic peak located at 3.16V is more intensive, indicating more Li<sup>+</sup> ions are extracted from the interstitial sites of MoO<sub>3</sub> lattice, and remarkable weakening of this peak in the following cycles suggests that the Li<sup>+</sup> ions are not able to insert the interstitial sites again. Compared to the pristine nanobelts, the cathodic and anodic current peaks located at 2.03V and 2.77V are much more intensive, which indicates that although the deintercalation of Li<sup>+</sup> ions causes the irreversible phase transformation of MoO<sub>3</sub> layers, the reversibility of Li<sup>+</sup> ions insertion/extraction between the layer is better than that of the pristine nanobelts.

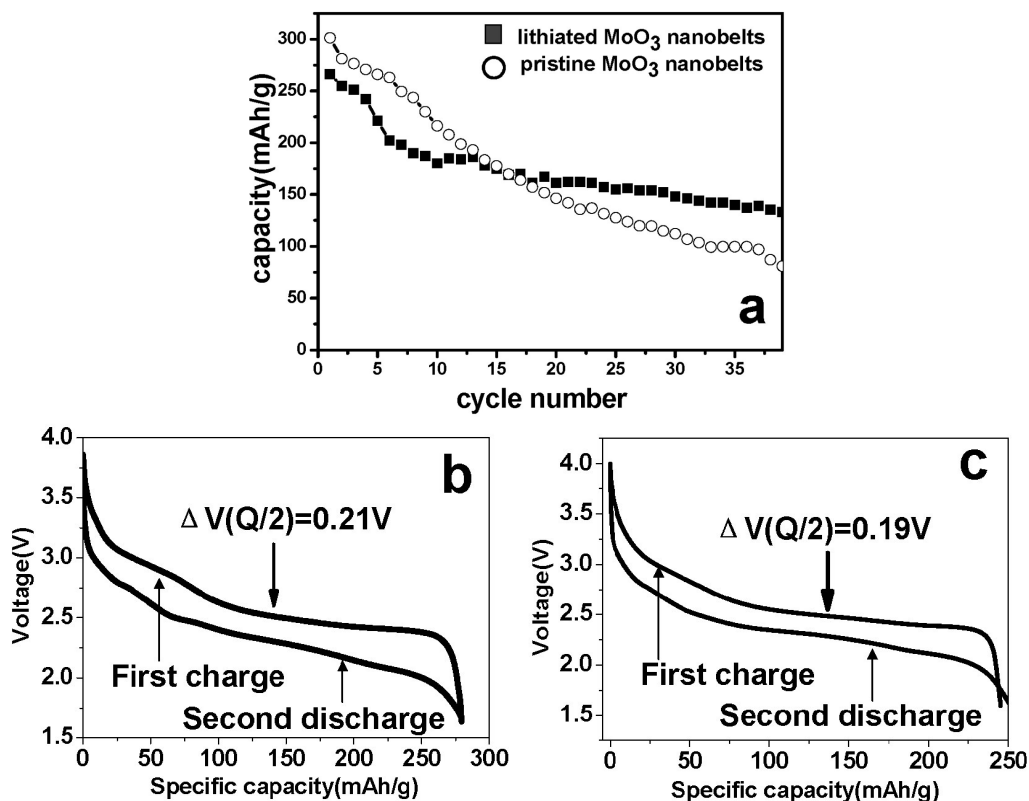


**Figure 4.** (a) Cycling property of pristine MoO<sub>3</sub> nanobelts and lithiated MoO<sub>3</sub> nanobelts. (b, c) Voltage hysteresis loops during the charge/discharge process for for pristine and lithiated MoO<sub>3</sub> nanobelts, respectively.

Fig. 4a shows the curves of discharge capacity vs the cycle number for the electrodes made from pristine and lithiated MoO<sub>3</sub> nanobelts at charge-discharge current density of 30 mA/g and temperature of 25 °C. It is apparent that the discharge capacity of pristine MoO<sub>3</sub> nanobelts decreases greatly with cycling, fading from 301 mAh/g in the first cycle to 81 mAh/g in the 39th cycle, corresponding to

capacity retention of 26.5%. Although the discharge capacity of lithiated MoO<sub>3</sub> nanobelts is 266 mAh/g in the first cycle, it still retains 133 mAh/g after 39 cycles, corresponding to about 50% of its first capacity. The discharge capacity of the lithiated MoO<sub>3</sub> nanobelts becomes lower probably because Li<sup>+</sup> ions had occupied some space of the interstitial sites during the hydrothermal reaction. In addition, although the capacity decreases fast in the first ten cycles, more stable cycles are obtained later. The intercalation of Li<sup>+</sup> ions into MoO<sub>3</sub> nanobelts significantly enhances the cycling stability and reversibility, probably the Li<sup>+</sup> ions which occupy the interstitial site of MoO<sub>3</sub> lattice stabilize the structure and reduce the electrostatic interaction between MoO<sub>3</sub> layer and Li<sup>+</sup> ions in interlayer during the discharge.

The voltage curves for the MoO<sub>3</sub> nanobelts exhibit an obvious hysteresis in the discharge/charge profiles (Fig. 4b,c). The hysteresis degree is determined by the difference between the potential during lithium insertion and extraction at the half reversible capacity  $\Delta(V(Q/2))$ . For the lithiated nanobelts,  $\Delta(V(Q/2))=0.19\text{V}$ , which is less than that of pristine nanobelts ( $\Delta(V(Q/2))=0.21\text{V}$ ), showing the lithiated nanobelts exhibit better insertion/extraction reversibility. All these results indicate that lithiated MoO<sub>3</sub> nanobelts are promising cathode materials in lithium ion batteries.

#### 4. CONCLUSIONS

Lithiation modification of MoO<sub>3</sub> nanobelts was conducted by a simple hydrothermal method. The length of the nanobelts decrease after lithiation, but the crystal structure and belt-shape morphology are kept. The directly lithiated MoO<sub>3</sub> nanobelts exhibit good cycling capability, with a capacity retention rate of 50% after 39 cycles, while the non-lithiated nanobelts retain only 26.5%. The improved electrochemical performance may be because the Li<sup>+</sup> ions occupy the interstitial site of MoO<sub>3</sub> lattice which can stabilize the structure and reduce the electrostatic interaction between MoO<sub>3</sub> layer and Li<sup>+</sup> ions in the interlayer during the cycling process.

#### ACKNOWLEDGEMENTS

This work was supported by the National Nature Science Foundation of China (50702039, 50672071, 50672072), the Key Project of Chinese MOE (105124), Program for Changjiang Scholars and Innovative Research Team in University (PCSIRT, No. IRT0547), MOE, China, the Foundation for Innovation Research Team (2005ABC004) and the Nature Science Foundation (2006ABA310) of Hubei Province, the Wuhan Youth Chenguang Project (20065004116-17).

#### References

1. L. Q. Mai, B. Hu, W. Chen, Y. Y. Qi, C. S. Lao, R. S. Yang, Y. Dai, Z. L. Wang, *Adv. Mater.* 19 (2007) 3712
2. T. A. Kerr, H. Wu, L. F. Nazar., *Chem. Mater.* 8 (1996) 2005.
3. Y. B. Li, Y. Bando, D. Goldberg, K. Kurashima, *Appl. Phys. Lett.* 81 (2002) 5048.
4. T. Caillat, J. P. Fleurial, G. J. Snyder, *Solid State Sci.* 1 (1999) 535.
5. K. T. Queeney, C. M. Friend, *J. Phys. Chem. B* 104 (2000) 409.
6. E. Comini, L. Yubao, Y. Brando, G. Sberveglieri, *Chem. Phys. Lett.* 407 (2005) 368.

7. R. Tenne, L. Margulis, M. Genut, G. Hodes, *Nature* 360 (1992) 444.
8. Z. Hussain, *J. Mater. Res.* 16 (2001) 2695.
9. X. L. Li, J. F. Liu, Y. D. Li, *Appl. Phys. Lett.* 81 (2002) 4832.
10. C. S. Johnson, D. W. Dees, M. F. Mansuetto, *J. Power Source* 68 (1997) 570.
11. P. A. Christian, J. N. Carides, F. J. DiSalvo, J. V. Waszczak, *J. Electrochem Soc.* 127 (1980) 2135.
12. T. Tsumura, M. Inagaki, *Solid State Ionics* 104 (1997) 183.